THE JOURNAL OF BIOLOGICAL CHEMISTRY VOL. 288, NO. 4, pp. 2210–2222, January 25, 2013

Netrin-1 Promotes Glioblastoma Cell Invasiveness and Angiogenesis by Multiple Pathways Including Activation of RhoA, Cathepsin B, and cAMP-response Element-binding Protein*

Received for publication, July 11, 2012, and in revised form, November 27, 2012 Published, JBC Papers in Press, November 29, 2012, DOI 10.1074/jbc.M112.397398

Akio Shimizu[‡§1] **Hironao Nakayama**[‡§¶1], **Priscilla Wang**[‡1], **Courtney König**[‡], **Tomoshige Akino**[‡§], **Johanna Sandlund**[‡], **Silvia Coma**[‡§], **Joseph E. Italiano, Jr.**[‡‖], **Akiko Mammoto**[‡§], **Diane R. Bielenberg**[‡§], **and Michael Klagsbrun**[‡§**2]

*From the ‡Vascular Biology Program and Departments of §Surgery and **Pathology, Boston Children's Hospital, Harvard Medical School, Boston, Massachusetts 02115, the ‖Department of Medicine, Hematology Division, Brigham and Women's Hospital, Boston, Massachusetts 02115, and the ¶Graduate School of Medicine and Proteo-Medicine Research Center, Ehime University, Shitsukawa, Toon, Ehime 791–0295, Japan*

Background: Netrins and their receptors play a role in cancer; however, the molecular mechanisms are not well understood.
Results: Netrin-1 promotes glioblastoma cell invasion and angiogenesis, and these activities are abrogated by cathepsin B inhibitor.
Conclusion: Netrin-1 plays a cathepsin B-dependent dual role in glioblastoma progression by promoting both invasiveness and angiogenesis.
Significance: Novel netrin-1 mechanisms include activation of RhoA, cathepsin B, and cAMP-response element-binding protein.

Glioblastomas are very difficult tumors to treat because they are highly invasive and disseminate within the normal brain, resulting in newly growing tumors. We have identified netrin-1 as a molecule that promotes glioblastoma invasiveness. As evidence, netrin-1 stimulates glioblastoma cell invasion directly through Matrigel-coated transwells, promotes tumor cell sprouting and enhances metastasis to lymph nodes *in vivo*. Furthermore, netrin-1 regulates angiogenesis as shown in specific angiogenesis assays such as enhanced capillary endothelial cells (EC) sprouting and by increased EC infiltration into Matrigel plugs *in vivo*, as does VEGF-A. This netrin-1 signaling pathway in glioblastoma cells includes activation of RhoA and cyclic AMP response element-binding protein (CREB). A novel finding is that netrin-1-induced glioblastoma invasiveness and angiogenesis are mediated by activated cathepsin B (CatB), a cysteine protease that translocates to the cell surface as an active enzyme and co-localizes with cell surface annexin A2 (ANXA2). The specific CatB inhibitor CA-074Me inhibits netrin-1-induced cell invasion, sprouting, and Matrigel plug angiogenesis. Silencing of CREB suppresses netrin-1-induced glioblastoma cell invasion, sprouting, and CatB expression. It is concluded that netrin-1 plays an important dual role in glioblastoma progression by promoting both glioblastoma cell invasiveness and angiogenesis in a RhoA-, CREB-, and CatB-dependent manner. Targeting netrin-1 pathways may be a promising strategy for brain cancer therapy.

Axon guidance molecules play a key role in brain development by guiding axon growth and neural cell migration in the nervous system (1, 2). They mediate wiring of the nervous system by acting as attractive or repulsive environmental cues. However, it has been observed recently that axon guidance factors also have non-neuronal properties, for example, regulating angiogenesis, tumor growth, and inflammation using similar molecular mechanisms as in the nervous system (3, 4). Prominent axon guidance factors include ephrins, semaphorins, slits and netrins, and their receptors. Our laboratory has previously analyzed class 3 semaphorins and their receptors, the neuropilins (5, 6). Semaphorin 3F (SEMA3F)[3] is a potent inhibitor of tumor angiogenesis, growth, and metastasis (7, 8). The invasive ability of tumor cells is a major contributor to metastatic potential and death from cancer. As an example, glioblastoma multiforme is highly aggressive and has a patient median survival time of approximately 1 year, due to the high propensity of its tumor cells to invade surrounding healthy brain tissue (9). Our goals are to delineate the mechanisms involved.

* This work was supported, in whole or in part, by National Institutes of Health Grants CA37392 and CA45548 from the NCI (to M. K.). H. N. is supported by the Strategic Young Researcher Overseas Visiting Program for Accelerating Brain Circulation (No. S2207 to Dr. Shigeki Higashiyama, Ehime University Proteo-Medicine Research Center), Japan Society for the Promotion of Science, Japan.
[1] These authors contributed equally to this work.
[2] To whom correspondence should be addressed: Karp Family Research Laboratories 12.210, 1 Blackfan Circle, Boston, MA 02115. Tel.: 617-919-2157; E-mail: michael.klagsbrun@childrens.harvard.edu.

[3] The abbreviations used are: SEMA, semaphorin; EC, endothelial cell; CREB, cyclic-AMP response element binding protein; CatB, cathepsin B; ANXA2, annexin A2; DCC, deleted in colorectal cancer; UNC5, uncoordinated 5; DSCAM, Down syndrome cell adhesion molecule; HUVEC, human umbilical vein endothelial cells; PFA, paraformaldehyde; qRT-PCR, quantitative real-time polymerase chain reaction; ERK, extracellular signal-regulated kinase; MAPK, mitogen-activated protein kinase; MEK, mitogen-activated protein kinase.

Netrins are laminin-like proteins first identified as axonal guidance molecules in the neural development of *Caenorhabditis elegans* (10). The netrin family consists of secreted axon guidance molecules that include netrin-1, netrin-3, and netrin-4 and these are composed of ~600 amino acids. Netrin family activity is mediated by several receptors, including uncoordinated 5A-D (UNC5A-D), deleted in colorectal cancer (DCC), its orthologue neogenin, and Down syndrome cell adhesion molecule (DSCAM). During brain development, floor plate-secreted netrin-1 diffuses and establishes a gradient to attract commissural axons expressing netrin receptors to the midline of the central nervous system (1, 10).

Netrin-1 also has a number of non-neuronal functions, for example, regulating angiogenesis (11–14), inflammation (15), and atherosclerosis (16). Additionally, netrin-1 has been identified recently as a novel stimulator of cancer cell invasion in melanoma and colorectal cancer (17, 18). In tumors, netrin-1 acts as an oncogene that is up-regulated in several cancers, such as metastatic breast cancer, non-small cell lung cancer, and pancreatic adenocarcinoma (19, 20). The netrin-1 receptor DCC was identified originally as a candidate tumor suppressor in colon cancer associated with a deletion in chromosome 18q21 (21, 22). DCC and other netrin-1 receptors are dependence receptors that trigger apoptosis in the absence of the netrin-1 ligand (23). Loss of netrin-1 receptor expression is associated with a poor prognosis in patients with colorectal tumors, glioblastoma, and breast carcinoma (24, 25).

Although it is clear that netrins and their receptors play a role in cancer, the detailed molecular mechanisms involved are not well understood. In particular, it is not clear which factors regulate glioblastoma invasiveness, a major contributor to the poor prognosis of glioblastoma patients. In this report, we demonstrate that netrin-1 has a dual role in glioblastoma progression. It stimulates glioblastoma cell invasion through Matrigel-coated transwells and enhances metastasis to lymph nodes *in vivo*. Invasiveness is dependent on the activation of the small GTPase RhoA and the activation of CREB, a transcription factor. As a novel feature, netrin-1-induced invasiveness is dependent on activation and translocation to the cell surface of CatB, a cysteine protease. In addition, netrin-1 is a potent angiogenic factor; it increases blood vessel infiltration into Matrigel plugs implanted into mice in a CatB-dependent manner. It is concluded that netrin-1 plays a dual role in glioblastoma progression by promoting glioblastoma cell invasiveness and stimulating angiogenesis. Targeting netrin-1 pathways may be a promising strategy for brain cancer therapy.

EXPERIMENTAL PROCEDURES

Antibodies and Reagents—The following antibodies were purchased from Cell Signaling Technology: rabbit monoclonal anti-RhoA antibody (number 2117); rabbit monoclonal anti-phospho-cofilin (Ser-3) antibody (number 3313); rabbit polyclonal anti-cofilin antibody (number 3312); rabbit monoclonal anti-phospho-CREB (Ser-133) antibody (number 4276); rabbit monoclonal anti-CREB antibody (number 9197); rabbit polyclonal anti-phospho-p44/42 MAPK (ERK1/2) (Thr-202/Tyr-204) antibody (number 9101); and mouse monoclonal anti-p44/42 MAPK (ERK1/2) antibody (number 4696). The mouse monoclonal anti-CatB antibody (ab58802) was from Abcam. The rabbit polyclonal anti-Annexin A2 antibody (H-50, sc-9061) was purchased from Santa Cruz Biotechnology, Inc. The mouse monoclonal anti-β-actin antibody (AC-15) and anti-CD31 antibody (number 550274) were from Sigma and BD Biosciences, respectively. The mouse Netrin-1 Affinity Purified Polyclonal antibody (AF1109) and the Human Phospho-Kinase Array Kit (ARY003) were obtained from R&D Systems. Phosphoproteins were detected according to the manufacturer's protocol. The MEK inhibitor (U0126) was purchased from EMD.

Cell Culture—U87MG cells, U87MG cell transfectants (clone numbers 21 and 24), U251, and U343 human glioblastoma cells were cultured in minimum essential medium (Invitrogen) containing 10% fetal bovine serum (FBS, Denville Scientific, Inc.) and 1% L-glutamine/penicillin G/streptomycin sulfate (Invitrogen) in a 10% CO_2 incubator at 37 °C. 293T cells were cultured in DMEM (Invitrogen) containing 10% FBS and 1% L-glutamine/penicillin G/streptomycin sulfate. Human umbilical vein endothelial cells (HUVEC) were purchased from Lonza and cultured in EGM2. Mouse brain EC were isolated as described in our previous report (26). 293T and EC cells were maintained in 5% CO_2 incubator at 37 °C.

Human Recombinant Netrin-1—A full-length netrin-1 construct was kindly provided by Dr. Anne Eichmann (Yale School of Medicine). Subcloned netrin-1 cDNA was introduced into a pcDNA3.1/V5-His-TOPO plasmid (Invitrogen). The netrin-1 construct was then transfected into 293T cells using FuGENE HD Transfection Reagent (Roche Applied Science) to express His- and V5-tagged netrin-1 protein. Netrin-1 secreted into culture medium was purified on HiTrap HP Chelating columns (GE Healthcare Bio-Sciences Corp.) as previously described (27). Recombinant human netrin-1 (number 6419-N1) was also purchased from R&D Systems.

F-actin Staining—Cells were fixed with 4% paraformaldehyde (PFA) followed by permeabilization with 0.2% Triton X-100 in phosphate-buffered saline (PBS). F-actin and nuclei were stained with Alexa Fluor 488 phalloidin (Invitrogen) and 4′,6-diamidino-2-phenyl-indole, dihydrochloride (DAPI, Invitrogen), respectively.

Migration and Invasion—Migration and invasion assays were performed in Transwells® (Corning Glass) with an 8.0-μm pore size and coated with 0.5% gelatin or BD Matrigel™ Basement Membrane Matrix (BD Biosciences) (0.1 mg/ml), respectively (8, 28). Cells that had migrated through the filters after 20 h at 37 °C were stained with a Diff-Quick cell staining kit (Dade Behring, Inc.), and five fields were counted by phase microscopy.

Spheroids—The preparation of spheroids was performed as previously described (28, 29). Briefly, cells were suspended and aggregated to form cellular spheroids (500 cells/spheroid) by hanging drop culture. Spheroids were embedded into collagen gels treated with netrin-1 protein. After 16 h incubation, spheroids were fixed with 4% PFA and permeabilized by 0.2% Triton X-100. F-actin and nuclei were stained with Alexa Fluor 488 phalloidin and DAPI, respectively. Fluorescent images from five to seven spheroids per experimental group were acquired

on a confocal microscope (Leica) and total sprout length and number of the sprouts were analyzed using ImageJ software.

RhoA Activity—RhoA activity assays were performed as previously reported by us (8) using the RhoA activation assay kit based on rhotekin pull-down according to the manufacturer's instructions (Cytoskeleton).

Western Blotting—Western blotting was performed as previously described by us (8). Each sample was separated by SDS-PAGE, and the gels were transferred to polyvinylidene fluoride membranes. The membranes were blocked with 4% skim milk in TBS-T (0.1% Tween 20 in Tris-buffered saline (TBS)) for 30 min, followed by incubation with primary antibodies. After washing with TBS-T, the membranes were incubated with appropriate horseradish peroxidase-conjugated secondary antibodies. Immunoreactivity was detected using ECL detection reagents.

Quantitative Real-time Polymerase Chain Reaction (qRT-PCR)—Total RNA was isolated using an RNeasy Kit (Qiagen). Reverse transcription of RNA was performed with SuperScript II Transcriptase (Invitrogen) according to the manufacturer's protocol. After first-strand synthesis, qRT-PCR was performed using the iQ SYBR Green Supermix mixture (Bio-Rad) with the ABI StepOnePlus Real-Time PCR Systems (Applied Biosystems). Each experiment was done in duplicate and repeated three times. The amount of mRNA expression was normalized to GAPDH. The qRT-PCR primers used in the present study are as follows: Netrin-1, 5′-TGCAAGAAGGACTATGCCGTC-3′ 5′-GCTCGTGCCCTGCTTATACAC-3′; DCC, 5′-GCCACAAACCAACAGAGGAT-3′ and 5′-GCTGCTTCATGAGTCCTTCC-3′; neogenin, 5′-ATGGTGACCAAAGGTCGAAG-3′ and 5′-AGTCACATCCTTGGGTGGAG-3′; DSCAM, 5′-TCCACCTCAGGAAGTTCACC-3′ and 5′-CCACGGATAATCCCATTTTG-3′; UNC5A, 5′-CCGGCTGATGATCCCTAATA-3′ and 5′-CTTGTGCAGCGTGAGGTAGA-3′; UNC5B, 5′-GAGGTGGAATGGCTCAAGAA-3′ and 5′-ATGAGGTTGTGGTCGATGGT-3′; UNC5C, 5′-AGCAAGGCAGACTGATCCAT-3′ and 5′-TCAGCAAGCTGACTCCTGAA-3′; UNC5D, 5′-AGTGGGTCCATCAGAACGAG-3′ and 5′-CATGGAAGTCCTCCACCTGT-3′; CatB, 5′-TATGCCACTGGTTTGCATTGCTGG-3′ and 5′-TGTACCTTGGCAGGACAGTGGAAT-3′; GAPDH, 5′-ACAGTCAGCCGCATCTTCTT-3′ and 5′-GCCCAATACGACCAAATCC-3′.

RNA Interference—Control siRNA (Silencer Negative Control #2 siRNA) was purchased from Applied Biosystems. CREB (#1: Hs_CREB1_5, #2: Hs_CREB1_6) siRNA were obtained from Qiagen. Transfection of siRNA (20 nM) was performed with siLentFect Lipid Reagent (Bio-Rad) according to the manufacturer's protocol.

Cathepsin B Activity—CatB fluorogenic substrate (cathepsin B detection kit, EMD) was used to visualize enzymatic activity. U87MG cells (6×10^4 cells/well in a 6-well plate) were cultured on coverslips and incubated with netrin-1 (200 ng/ml) for 3 h. The cells were subsequently incubated for 1 h with the CatB fluorogenic substrate. Hoechst 33342 (1 μg/ml) was added to the living cells and incubated for 5 min to stain the nuclei. Cells were fixed with 4% PFA and incubated with anti-CatB antibody. The samples on coverslips were mounted on glass slides and imaged by confocal microscopy. For inhibitor assays, cells were treated with the following cathepsin inhibitors (10 μM): leupeptin (Sigma), CatB inhibitor (CA-074Me, Sigma), CatD inhibitor (Pepstatin A, Calbiochem), CatL inhibitor VI (Calbiochem), or CatS inhibitor (Calbiochem). DMSO was used as a control.

Endothelial Tube Formation—HUVECs were cultured in EBM2 medium (Lonza) containing 0.5% FBS overnight. One million cells were seeded into a Matrigel-coated 24-well plate with 0.5% FBS/EBM2 medium in the absence or presence of netrin-1, followed by incubation for 16 h. The images were captured using an Eclipse TE300 microscope (Nikon). The number of tube junctions/area was quantified by using ImageJ software.

Matrigel Plugs—Matrigel plug assays were carried out as previously described (30). In brief, Matrigel plugs containing sphingosine 1-phosphate (1 μM), netrin-1 (16 μg/ml), or VEGF-A (5 μg/ml) were cast in cylindrical 4×4 mm (internal diameter x height) polydimethylsiloxane molds and incubated at 37 °C for 1 h before being implanted subcutaneously on the dorsa of C57BL/6 mice (8 weeks). In addition, 100 μM CatB inhibitor and CatD inhibitor were mixed with netrin-1 in the Matrigel plug. After 7 days, polydimethylsiloxane molds containing the gel plugs were collected, fixed with 4% PFA, and cryosectioned. H&E staining and immunostaining with anti-CD31 antibody were performed on cryosections. Blood vessel infiltration was evaluated by measuring CD31 positive cells in five different areas. Individual cell nuclei were identified by DAPI staining.

Metastasis—U87MG glioblastoma cells (parental or clone #21 which overexpresses netrin-1) were injected subcutaneously on the upper dorsum of (9 weeks, female) nude mice (10^6 cells per 100 μl of Hank's balanced salt solution), 5 mice per group in each protocol. To examine metastasis, primary tumors were resected after they reached 10 mm in diameter. After 1 month post-resection, the inguinal and axial lymph nodes were removed and were fixed and embedded in paraffin. Paraffin-embedded sections were deparaffinized using xylene and a graded series of ethanol (100, 90, and 80%). Sections were immunostained with monoclonal mouse anti-human Ki-67 antibody (MIB-1) or monoclonal mouse anti-proliferating cell nuclear antigen antibody (Dako). The metastatic lesion sizes (diameter) were measured in the various lymph nodes. Metastatic lesions of 50 μm or less were considered to be negative.

Statistical Analysis—All assays were independently performed three times. The results are represented as mean ± S.D. The two groups were compared using the Student's *t* test. $p < 0.05$ was considered statistically significant.

RESULTS

Netrin-1 Induces Glioblastoma Cell Migration, Invasion, and Metastasis—Glioblastoma tumors are highly invasive in the brain. To determine whether netrin-1 contributes to glioblastoma cell migration and invasiveness, transwells coated with gelatin (migration) or Matrigel (invasion) assays were carried out in three glioblastoma cell lines, U87MG, U251, and U343. Netrin-1 induced migration and invasion of these cell lines in a dose-dependent manner (Fig. 1*A*). There were variations among the cell lines in basal activity; nevertheless, netrin-1-induced activity in general was increased 3–4-fold. U87MG cells overexpressing netrin-1 (stable clones 21 and 24) were prepared (Fig. 1*B*). Western blot analysis showed that these

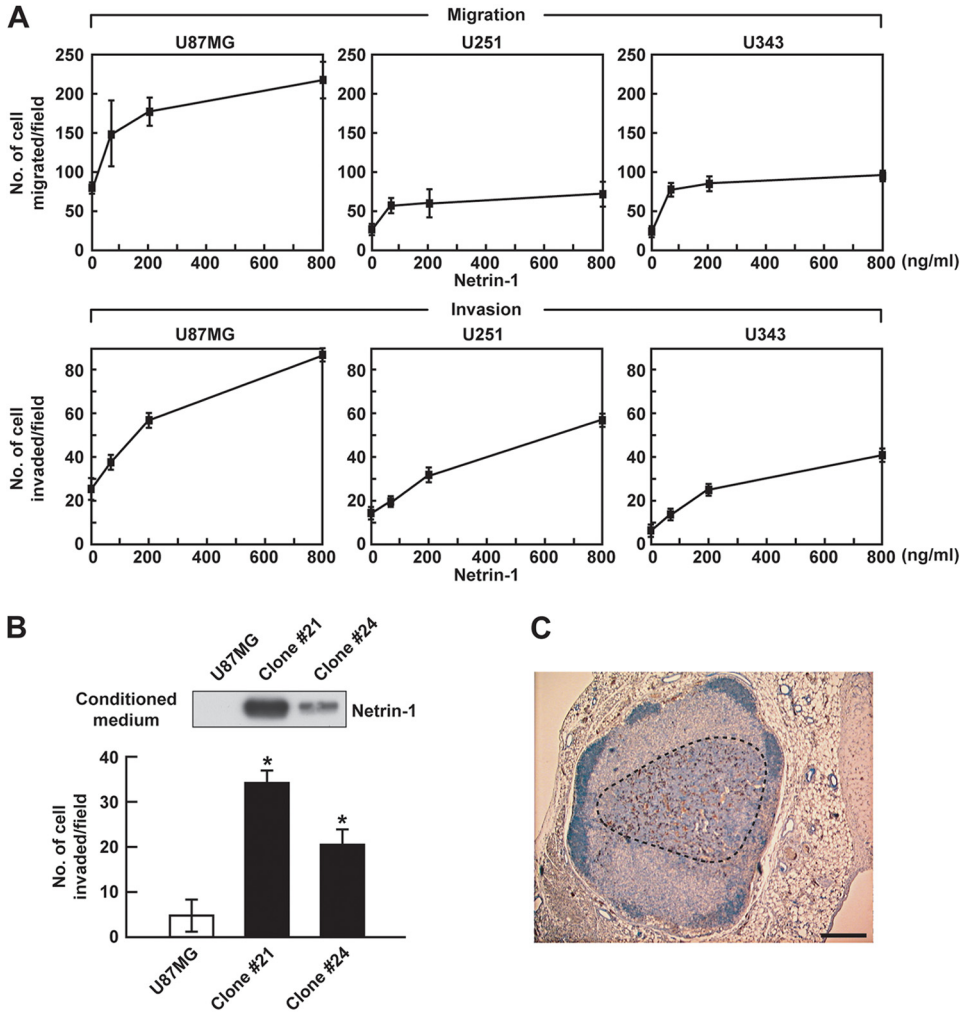

FIGURE 1. **Netrin-1 induces glioblastoma cell migration and invasiveness.** *A*, glioblastoma cells were treated with netrin-1 (0–800 ng/ml) and assessed for their ability to migrate and invade through 0.5% gelatin or Matrigel-coated transwells. *B*, parental U87MG cells and netrin-1 stable clones (21 and 24) were assessed for their ability to invade through Matrigel-coated transwells. Conditioned medium was analyzed by Western blotting with anti-netrin-1 antibody. Data represent the mean ± S.D. ($n = 3$), *, $p < 0.05$. *C*, representative image of metastasis into an inguinal lymph node. U87MG cells overexpressing netrin-1 (*clone 21*) were subcutaneously implanted in nude mice. After 1 month post-resection, the inguinal and axial lymph nodes were isolated. Staining for human-specific Ki-67 identified U87MG cells that had metastasized to the nodes (see areas enclosed by *black dotted lines*). A metastatic lesion of 700 μm was observed in netrin-1 clone #21 group. The *scale bar* indicates 200 μm.

clones expressed substantial netrin-1 compared with parental cells. In addition, overexpression of netrin-1 was correlated with increased invasiveness, 6- and 4-fold for clones 21 and 24, respectively, compared with parental cells (Fig. 1*B*). In control mice, 5 of 20 lymph nodes had metastatic lesions. On the other hand, in U87MG cells overexpressing netrin-1 (clone 21), all 20 lymph nodes, including inguinal and axial, displayed metastatic lesions (Table 1). A representative metastatic lesion of 700 μm in diameter is shown in Fig. 1*C*. Together, these results show that netrin-1 is active as an invasive factor *in vitro* and *in vivo*.

TABLE 1

Incidence of lymph node metastasis

U87MG cells or U87MG cells overexpressing netrin-1 (clone 21) were implanted subcutaneously on the dorsal flank of nude mice, 5 mice per group in each protocol. Primary tumors were resected after they reached a size of 10 mm in diameter. After 1 month post-resection, the inguinal and axial lymph nodes were removed and immunostained with anti-PCNA antibody.

Tumor type	LN1[a]	LN2[b]	LN3[c]	LN4[c]
U87MG	3/5	1/5	1/5	0/5
Netrin-1 (clone 21)	5/5	5/5	5/5	5/5

[a] LN1, the sentinel or draining inguinal lymph node.
[b] LN2, the contralateral inguinal lymph node.
[c] LN3 and LN4 refer to axial lymph nodes. Metastatic lesion size of 50 μm or less in diameter was considered as negative.

Netrin-1 Promotes Angiogenesis—Glioblastomas are highly vascularized tumors that express high levels of VEGF, a potent angiogenesis factor (9). Netrin-1 is a pro-angiogenic factor, as shown in invasion, sprouting, tube formation, and Matrigel plug assays (Fig. 2). Netrin-1 stimulated early passage mouse brain EC invasion in a dose-dependent manner, with a 2-fold increase at the peak dose of 200 ng/ml (Fig. 2*A*). There was an 8–10-fold increase in mouse brain EC sprouting (Fig. 2*B*). Some individual EC migrated out of the netrin-1-treated spheroids (Fig. 2*B*, *arrowhead*), indicating that the sprouting assay measured both migration and sprouting. As an additional angiogenesis *in vitro* assay, netrin-1 induced HUVEC tube formation (Fig. 2*C*). The effects of netrin-1 on angiogenesis *in vivo* were measured in the Matrigel plug assay. Matrigel was mixed with either netrin-1 nor VEGF-A and the Matrigel plugs were implanted into C57BL/6 mice. Netrin-1-treated Matrigel plugs

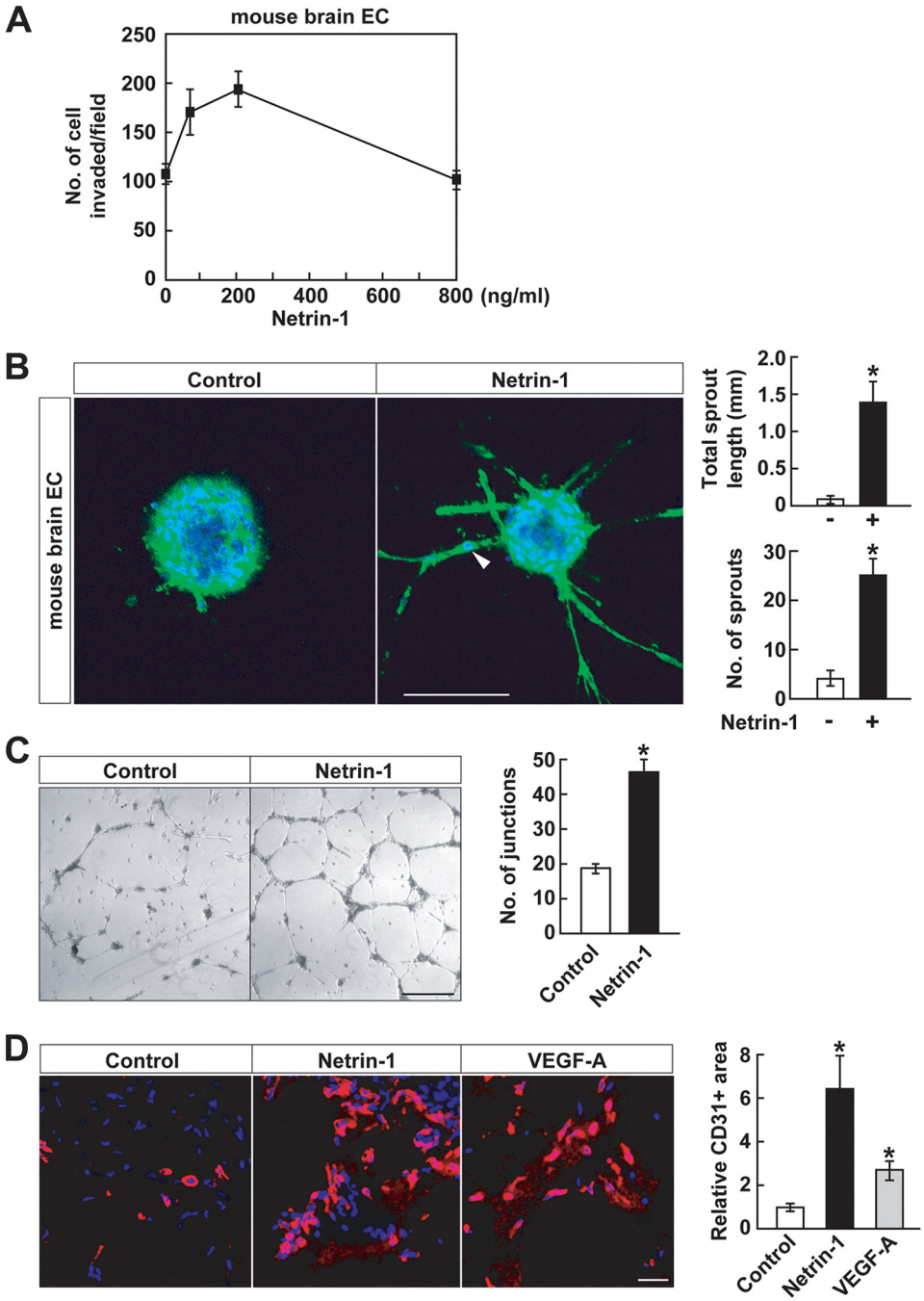

FIGURE 2. **Netrin-1 promotes angiogenesis.** *A*, mouse brain EC were treated with netrin-1 (0–800 ng/ml) and assessed for their ability to invade through Matrigel-coated transwells. *B*, mouse brain EC spheroids were stained with Alexa Fluor 488 phalloidin and DAPI and assessed for total sprout length and sprout number in the absence or presence of netrin-1 (400 ng/ml). Data represent the mean ± S.D. ($n = 3$), *, $p < 0.05$. The *scale bar* indicates 100 μm. *Arrowhead* indicates migrating EC from spheroid. *C*, HUVEC were seeded on the Matrigel-coated well plate in the presence or absence of netrin-1 (400 ng/ml). The number of tube junctions/area was measured by ImageJ software. Data represent the mean ± S.D. ($n = 3$), *, $p < 0.05$. The *scale bar* indicates 100 μm. *D*, Matrigel plugs, either left untreated or mixed with netrin-1 (16 μg/ml) or VEGF-A (5 μg/ml), were implanted into C57BL/6 mice. After 7 days, Matrigel plugs were removed and frozen sections were stained with anti-CD31 antibody and DAPI. CD31 positive cells were measured using ImageJ software. Data represent the mean ± S.D. ($n = 3$), *, $p < 0.05$. The *scale bar* indicates 10 μm.

displayed 6-fold increased infiltration of CD31-positive EC compared with control plugs. There was also a 3-fold infiltration to Matrigel plugs containing VEGF-A, a potent angiogenesis factor, which served as a positive control (Fig. 2*D*). Together, these *in vitro* and *in vivo* results indicate that netrin-1 is an active angiogenic factor.

Netrin-1 Activates RhoA—Confocal microscopy showed that netrin-1 altered U87MG cell and HUVEC morphology; for example, there was a 2–4-fold increase in F-actin stress fiber formation in both U87MG cells and HUVEC compared with control (Fig. 3*A*, *b* and *f versus a* and *e*). This netrin-1 effect was inverse to that of SEMA3F, which reduced stress fiber formation, thereby collapsing the F-actin cytoskeleton (Fig. 3*A*, *c* and *g*). The small GTPase RhoA regulates F-actin polymerization, cell contractility, and stress fiber formation (31, 32). By using a rhotekin pull-down assay, it was found that netrin-1 activated

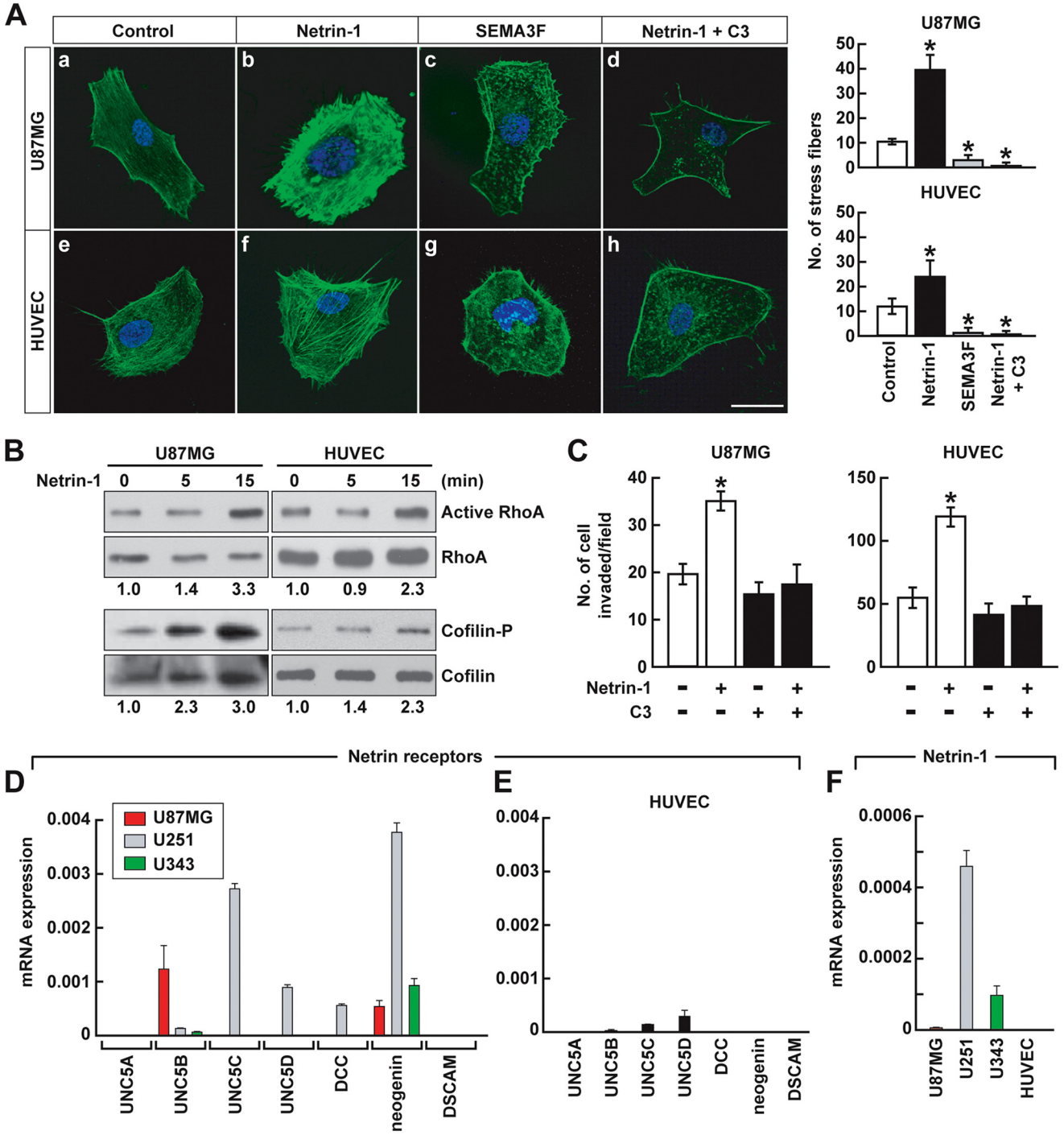

FIGURE 3. **Netrin-1 activates RhoA and inhibits cofilin.** *A*, U87MG cells and HUVEC were treated with netrin-1 (200 ng/ml) or SEMA3F (640 ng/ml). After 45 min, cells were fixed and stained with Alexa Fluor 488 phalloidin and DAPI, and observed by confocal microscopy. To inhibit RhoA, cells were incubated with the RhoA inhibitor C3 transferase (1 μg/ml) followed by 2 h of netrin-1 treatment. The number of stress fibers was counted. Data represent the mean ± S.D. (n = 3), *, $p < 0.05$. The *scale bar* indicates 20 μm. *B*, U87MG cells and HUVEC were treated with netrin-1 (200 ng/ml) for 0–15 min. For detection of RhoA activity, cell lysates were pulled down with rhotekin beads, followed by Western blotting with anti-RhoA antibody. Total cell lysates were analyzed by Western blotting with anti-RhoA or anti-cofilin. The intensity of active RhoA and phosphorylated cofilin bands was normalized to their respective total RhoA and cofilin and the *numbers below* gel lanes represent the fold-change in intensity relative to 0 min. *C*, U87MG cells and HUVEC were treated with or without C3 transferase with or without the addition of netrin-1 (200 ng/ml), and assessed for their ability to invade with Matrigel-coated transwells. Data represent the mean ± S.D. (n = 3), *, $p < 0.05$. *D* and *E*, Netrin-1 receptor mRNA levels were measured in three glioblastoma cell lines (*D*) and HUVEC (*E*). mRNA levels were normalized to GAPDH mRNA. Data represent the mean ± S.D. (n = 3). *F*, netrin-1 mRNA levels were measured in three glioblastoma cell lines and HUVEC. mRNA levels were normalized to GAPDH mRNA. Data represent the mean ± S.D. (n = 3).

RhoA within 15 min in both cell types (Fig. 3*B*), stabilizing the F-actin cytoskeleton. Cofilin (actin depolymerization factor) is a protein downstream from RhoA (31). RhoA activated by netrin-1 induced rapid phosphorylation of cofilin (Fig. 3*B*). Phosphorylated cofilin is an inactive form of cofilin. A specific RhoA inhibitor, C3 transferase, inhibited netrin-1-induced

U87MG cell and HUVEC stress fiber formation (Fig. 3*A*, *d* and *h*) and invasion (Fig. 3*C*), confirming that netrin-1 induces U87MG cell and HUVEC morphological changes and invasion via a RhoA and cofilin pathway. On the other hand, consistent with the collapsing activity of SEMA3F, RhoA was inactivated and cofilin was activated (8).

The differential responses of glioblastoma cells to netrin-1 might be a function of differential netrin-1-receptor expression (Fig. 3*D*). mRNA measurements by qRT-PCR of the seven presently known netrin-1 receptors revealed that neogenin alone was detected in all three glioblastoma cell lines. U87MG cells expressed UNC5B predominantly. However, we did not detect significant expression of netrin receptors in HUVEC (Fig. 3*E*). Netrin-1 expression was also measured. It was detected in glioblastoma cells, however, netrin-1 expression in HUVEC were below detection levels (Fig. 3*F*). It was concluded that glioblastoma cells but not HUVEC are a possible source of netrin-1 and netrin receptors.

Netrin-1-induced Invasiveness and Angiogenesis Are CatB-dependent—Glioblastoma is highly invasive in the brain, and it has been suggested that these cells express proteases that degrade matrix, thus facilitating invasion (9). One possibility is that matrix metalloproteinases are involved. However, a broad matrix metalloproteinase inhibitor, GM6001, had no effect on glioblastoma cell invasion (data not shown). On the other hand, leupeptin, a cysteine protease inhibitor, completely inhibited netrin-1-induced U87MG cell invasion (Fig. 4*A*). The cathepsin family contains up to 12 proteases, some of which have been implicated in glioblastoma invasive activity (33, 34). Inhibitors of CatB and, to a lesser degree, of CatS significantly inhibited netrin-1-induced U87MG cell invasion, whereas inhibitors of CatD and CatL had no effect (Fig. 4*B*). Netrin-1 increased CatB mRNA expression after 2 h (Fig. 4*C*). At the protein level, pro-CatB was processed in response to netrin-1 into 25/26- and 31-kDa CatB mature forms (Fig. 4*D*). In addition, netrin-1 induced CatB enzymatic activity as measured with a CatB-specific fluorogenic substrate, and this activity was inhibited by the specific CatB inhibitor CA-074Me (Fig. 4*E*). Netrin-1 induced U87MG cell sprouting that was completely inhibited by CatB inhibitor (Fig. 4*F*). The angiogenic effects of CatB were measured in the Matrigel plug assay. Netrin-1 induced CD31 positive blood vessel recruitment nearly 4-fold, which was abrogated by the CatB inhibitor but not the CatD inhibitor (Fig. 4*G*). Together, these results demonstrate that netrin-1 induces glioblastoma cell invasiveness and angiogenesis in a specific CatB-dependent manner.

Netrin-1 Induces Translocation of CatB to the Cell Surface—CatB is a lysosomal protein, so how can it act as a cell surface or secreted protease? Several studies have demonstrated that CatB exhibits aberrant localization to the cell membrane in several different cancer lines and also have suggested that this change in localization facilitates cell invasion through the extracellular matrix (35, 36). Netrin-1 induced CatB enzymatic activity in U87MG cells in a time course of 0–4 h (Fig. 5*A*, *a-c*). To detect cell surface-CatB by immunostaining, the U87MG cells were not membrane-permeabilized (Fig. 5*A*, *e-g*). The fluorogenic substrate used for staining was small enough to penetrate cell membranes without permeabilization. The merged images showed co-localization of enzymatically active CatB with cell surface-CatB protein (Fig. 5*A*, *i-k*). To show that CatB was cell surface-associated, we found that, in response to netrin-1, cell surface CatB co-localized with a calcium-dependent phospholipid-binding protein, ANXA2, a cell surface protein (Fig. 5*B*). This result is consistent with previous reports showing that ANXA2 was associated with CatB on the surface of tumor cells without netrin-1 involvement (35, 37). Together, these results demonstrate that netrin-1 stimulates translocation of an enzymatically active form of CatB to the cell surface. The netrin-1-induced translocation of CatB to the cell surface was abrogated by a RhoA inhibitor C3 transferase, indicating that netrin-1-induced CatB activation and translocation were dependent on RhoA activation (Fig. 5*A*, *d*, *h*, and *l*).

CREB Regulates Netrin-1-induced Glioblastoma Cell Invasiveness—A phosphoprotein antibody array was used to investigate the molecular mechanisms underlying netrin-1 activity in glioblastoma cells. Netrin-1 induced phosphorylation of ERK and CREB in U87MG cells (Fig. 6*A*). Immunoblotting experiments confirmed that netrin-1 activated CREB phosphorylation in a dose- and time-dependent manner, as well as ERK phosphorylation in a time-dependent manner (Fig. 6*B*). Inhibition of the MAPK pathway with MEK inhibitor U0126 suppressed netrin-1-induced CREB phosphorylation, indicating that netrin-1 activates CREB via the MAPK pathway (Fig. 6*C*). CREB is a basic/leucine zipper transcription factor that regulates cell invasion and metastasis of tumors (38, 39). To assess the effect of CREB on glioblastoma cell invasion, endogenous CREB was silenced by 2 siRNAs (labeled 1 and 2), both of which reduced CREB expression by 80–90% in U87MG cells (Fig. 6*D*). Knockdown of CREB inhibited U87MG cell invasion (Fig. 6*E*) and sprouting (Fig. 6*F*), induced by netrin-1. Moreover, netrin-1-induced CatB expression was suppressed by CREB knockdown (Fig. 6*G*). These results suggest that CREB regulates netrin-1-induced glioblastoma cell invasiveness by regulating CatB expression.

DISCUSSION

Brain tumors such as glioblastoma are highly invasive and vascular (9). Our primary goal in this study was to identify molecular factors that induce invasiveness and angiogenesis, key contributors to the aggressiveness of these tumors. We found that netrin-1, a regulator of axon guidance, plays a dual role in promoting glioblastoma invasiveness: (i) netrin-1 acts directly on glioblastoma cells to induce invasion through Matrigel and to enhance lymph node metastasis; and (ii) netrin-1 acts directly on EC to stimulate angiogenesis. Netrin-1 was shown previously to regulate tumor progression and angiogenesis (11–14, 17, 18); however, the underlying mechanisms are not well delineated. We identified three factors that contribute to the aggressive phenotype when activated by netrin-1; these include RhoA, CatB, and CREB.

Tumor cell invasiveness in response to netrin-1 was ascertained by measuring cell invasion through transwells coated with Matrigel *in vitro* and by analyzing tumor metastasis *in vivo*. Netrin-1 enhanced transwell invasion in three glioblastoma cell lines. In addition, stable clones overexpressing netrin-1 displayed a markedly increased basal invasion. One of these clones, when injected subcutaneously into mice, promoted the incidence of lymph node metastasis.

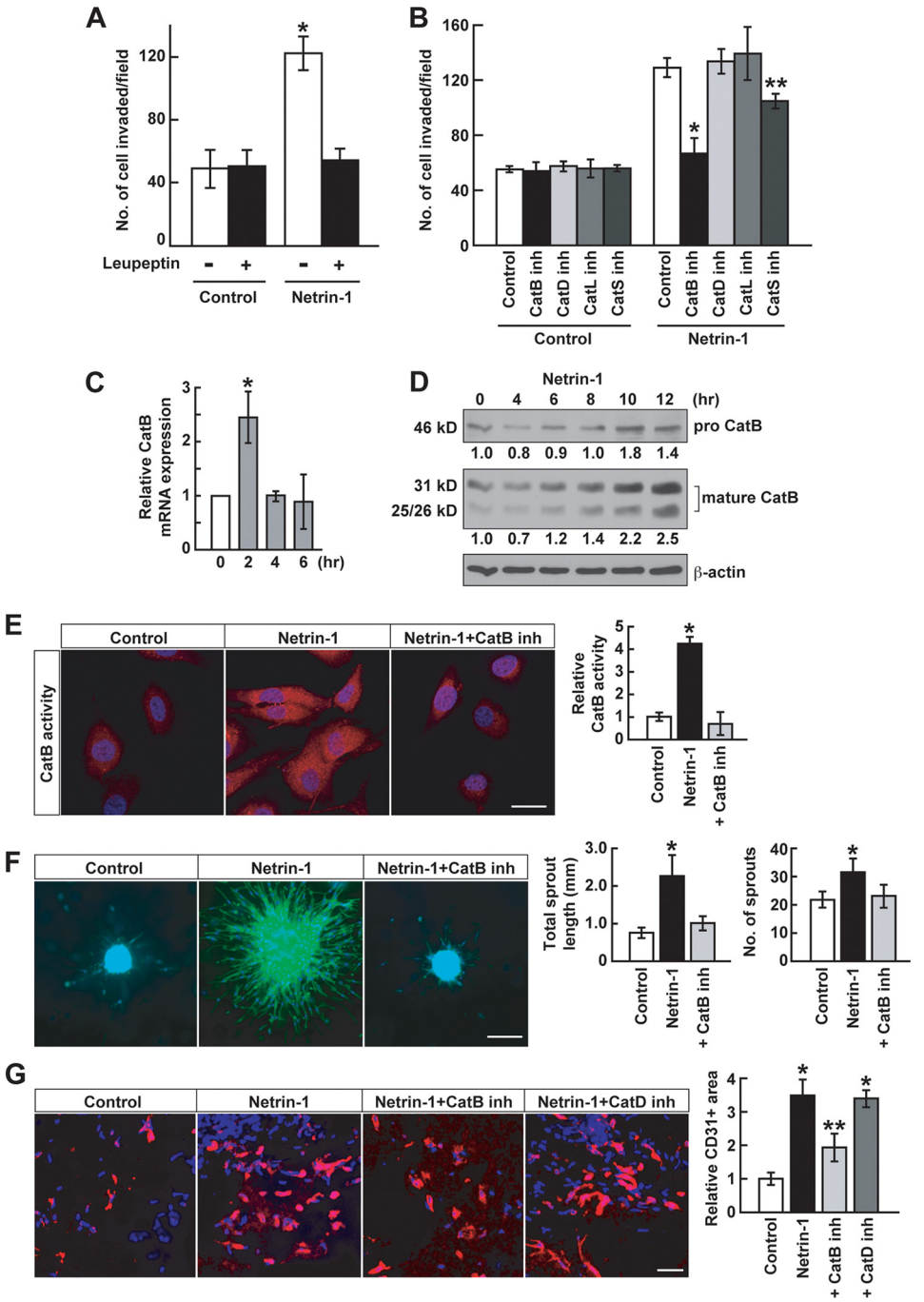

FIGURE 4. **Netrin-1-induced invasiveness and angiogenesis are CatB-dependent.** *A*, netrin-1-induced U87MG cell invasiveness was assessed with Matrigel-coated transwells. Cells were treated with a cysteine protease inhibitor, leupeptin (10 μM), with or without netrin-1 (200 ng/ml). Data represent the mean ± S.D. ($n = 3$), *, $p < 0.05$. *B*, U87MG cells were treated with 10 μM of inhibitors of CatB, CatD, CatL, or CatS with or without netrin-1 (200 ng/ml). Data represent the mean ± S.D. ($n = 3$), *, $p < 0.01$; **, $p < 0.05$. *C*, U87MG cells were treated with netrin-1 (200 ng/ml). Cells were collected at the indicated time points. CatB mRNA levels were analyzed by qRT-PCR. Data represent the mean ± S.D. ($n = 3$), *, $p < 0.05$. *D*, U87MG cells were treated with netrin-1 (200 ng/ml). Cells were collected at the indicated time points. Protein levels of pro- and mature forms of CatB were detected by Western blotting. The intensity of pro- and mature CatB bands was normalized to their respective β-actin controls and the *numbers below* gel lanes represent the fold-change in intensity relative to 0 min. *E*, U87MG cells were treated with netrin-1 (200 ng/ml) in the absence or presence of CatB inhibitor (10 μM). After 4 h, a fluorogenic CatB-specific substrate was used to measure CatB enzymatic activity (red fluorescence). The intensity of red fluorescence was measured using ImageJ software. Data represent the mean ± S.D. ($n = 3$), *, $p < 0.05$. The *scale bar* indicates 10 μm. *F*, U87MG cell spheroids implanted into collagen gels were stimulated with netrin-1 (200 ng/ml) in the absence or presence of CatB inhibitor (10 μM). Spheroids were stained with Alexa Fluor 488 phalloidin and DAPI and assessed for total sprout length and sprout number. Data represent the mean ± S.D. ($n = 3$), *, $p < 0.05$. The *scale bar* indicates 100 μm. *G*, netrin-1-induced EC infiltration into Matrigel plugs was abrogated by 10 μM CatB inhibitor but not by CatD inhibitor. Data represent the mean ± S.D. ($n = 3$), *, $p < 0.05$ *versus* control group; **, $p < 0.05$ *versus* group treated with netrin-1 alone. The *scale bar* indicates 10 μm.

Angiogenesis in response to netrin-1 was measured in several ways, including transwell invasion of capillary EC sprouting from spheroids embedded into three-dimensional collagen matrices, tube formation, and Matrigel plug blood vessel recruitment. To measure sprouting, early passage mouse brain EC were isolated with anti-CD31 antibody (26). Netrin-1

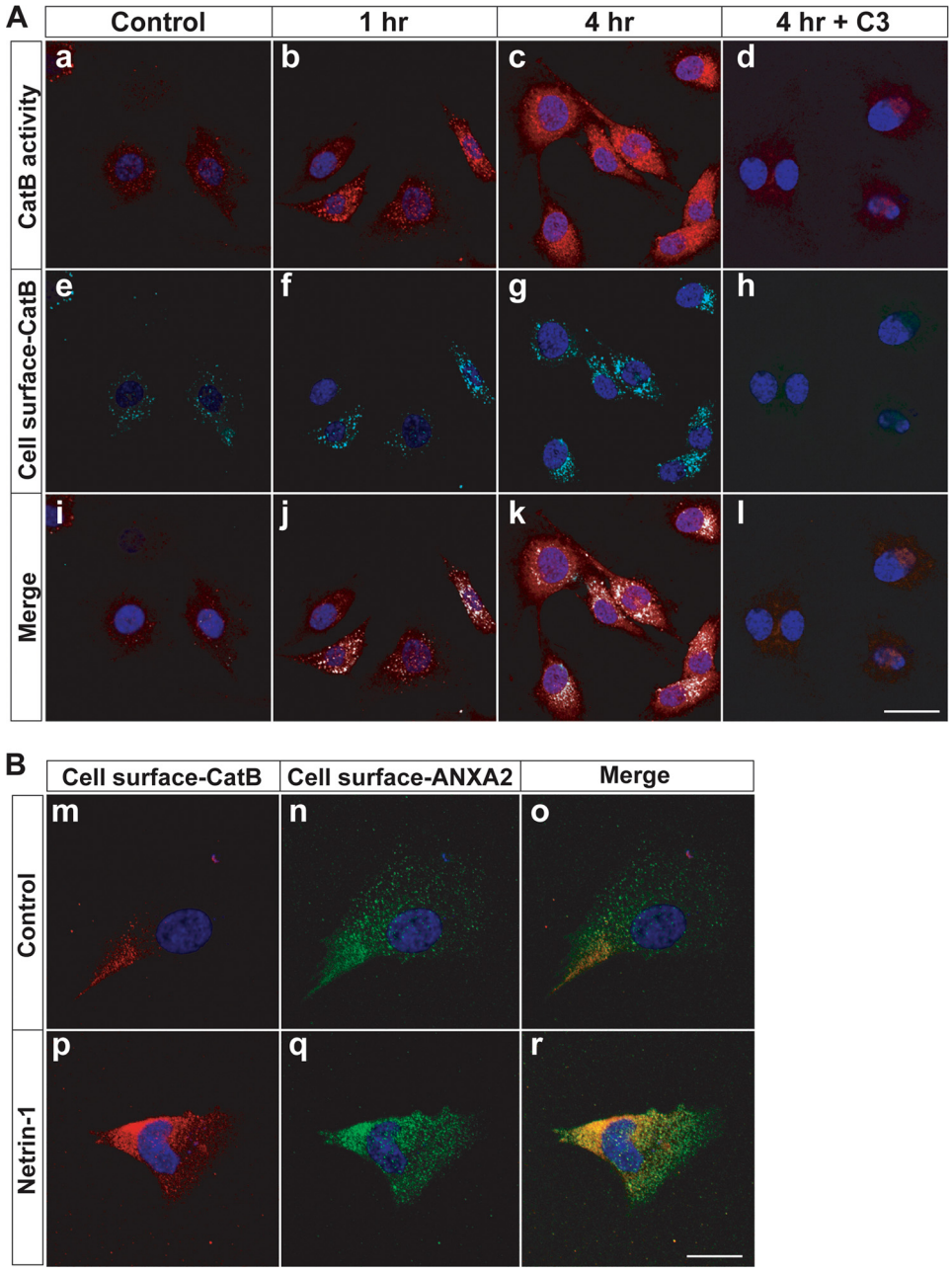

FIGURE 5. **Netrin-1 induces the translocation of CatB to the cell surface.** *A*, U87MG cells were incubated with netrin-1 (200 ng/ml). *a-d*, cells were treated with a fluorogenic CatB-specific substrate to measure CatB enzymatic activity (*red fluorescence*) at the indicated time point. *e-h*, the same cells (non-permeabilized) were stained for cell surface-CatB (*cyan fluorescence*) and nuclei (DAPI, *blue fluorescence*). Merged images are shown in *i-l*. Cells were treated with C3 transferase (1 μg/ml) prior to 2 h of netrin-1 treatment (*d, h,* and *l*). The *scale bar* indicates 10 μm. *B*, U87MG cells were incubated with netrin-1 (200 ng/ml) for 4 h. Cells (non-permeabilized) were stained for cell surface CatB (red fluorescence: *m* and *p*), cell surface ANXA2 (green fluorescence: *n* and *q*), and nuclei (DAPI, *blue fluorescence*). Merged images are shown in *o* and *r*. The *scale bar* indicates 10 μm.

induced a strong enhancement of thin, very elongated sprouts, about a 6–8-fold increase in sprout number. The sprouts contained EC that had migrated out of the spheroids, indicating that the sprouting assay detects migration as well. Angiogenesis was measured *in vivo* in a Matrigel plug assay. A Matrigel mold containing netrin-1 was implanted into C57BL/6 mice. After 1 week, there was a 6-fold increase in CD31 positive infiltrating cells. VEGF-A also induced CD31-positive EC serving as a positive control. Taken together, we suggest that netrin-1 plays an important dual role in glioblastoma progression by promoting glioblastoma cell invasiveness and angiogenesis.

However, whether netrin-1 is a promoter or inhibitor of angiogenesis is a matter of controversy. Our findings that netrin-1 is an inducer of angiogenesis are consistent with several studies demonstrating the pro-angiogenic effects of netrin-1 (13, 14). For example, netrin-1 induced proliferation and migration of EC in wound healing (13). Additionally, knockdown of *netrin-1a* in zebrafish inhibited vascular sprouting. Netrins accelerated neovascularization and reversed neuropathy and vasculopathy in murine models of ischemia (14). However, netrin-1 has also been shown to inhibit angiogenesis, for example, inhibition of Matrigel neovascularization by

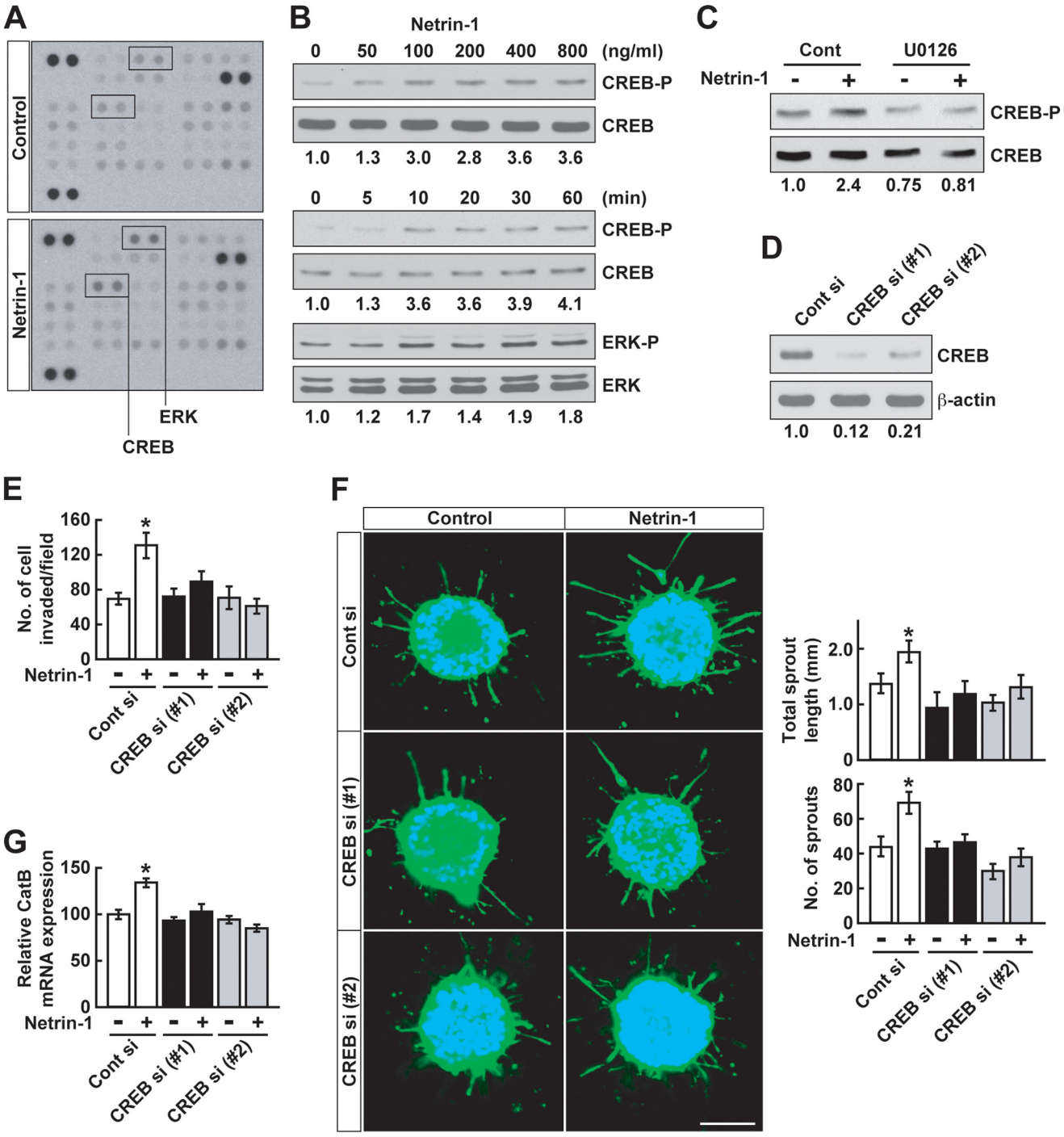

FIGURE 6. **Netrin-1 induces CREB phosphorylation.** *A*, U87MG cells were treated with netrin-1 (200 ng/ml). After 30 min, cell lysates were collected and applied to a phosphoantibody array as described under "Experimental Procedures." *B*, U87MG cells were treated with netrin-1 for 30 min at the indicated dose (*upper panels*). Cells were treated with netrin-1 (400 ng/ml) and lysates were collected at the indicated time points and Western blotted with anti-CREB or anti-ERK antibody (*lower panels*). The intensity of phosphorylated CREB and ERK bands was normalized to their respective total CREB and ERK, and the *numbers below* gel lanes represent the fold-change in intensity relative to control. *C*, U87MG cells were treated with U0126 (10 μM) prior to 30 min of netrin-1 treatment. Cells were collected and analyzed by Western blotting. The intensity of phosphorylated CREB bands was normalized to their respective total CREB and the *numbers below* gel lanes represent the fold-change in intensity relative to control. *D*, U87MG cells were transfected with control or CREB-specific siRNA (*#1* and *#2*) (20 nM). After 24 h, the silencing effect of CREB siRNA on CREB protein was analyzed by Western blotting. The intensity of CREB bands was normalized to their respective β-actin controls and the *numbers below* gel lanes represent the fold-change in intensity relative to controls. *E*, U87MG cells were transfected with control or CREB-specific siRNA (*#1* and *#2*) (20 nM). After 24 h, cells were treated with netrin-1 (400 ng/ml) and assessed for their ability to invade through Matrigel-coated transwells. Data represent the mean ± S.D. ($n = 3$), *, $p < 0.05$. *F*, U87MG cells were transfected with control or CREB-specific siRNA (20 nM). Spheroids were stimulated with netrin-1 (400 ng/ml) and stained with Alexa Fluor 488-phalloidin and DAPI and assessed for total sprout length and sprout number. Data represent the mean ± S.D. ($n = 3$), *, $p < 0.05$. The *scale bar* indicates 100 μm. *G*, U87MG cells were transfected with control or CREB-specific siRNA (*#1* and *#2*) (20 nM). Cells were treated with netrin-1 (400 ng/ml) for 2 h and CatB mRNA levels were analyzed by qRT-PCR. Data represent the mean ± S.D. ($n = 3$), *, $p < 0.05$.

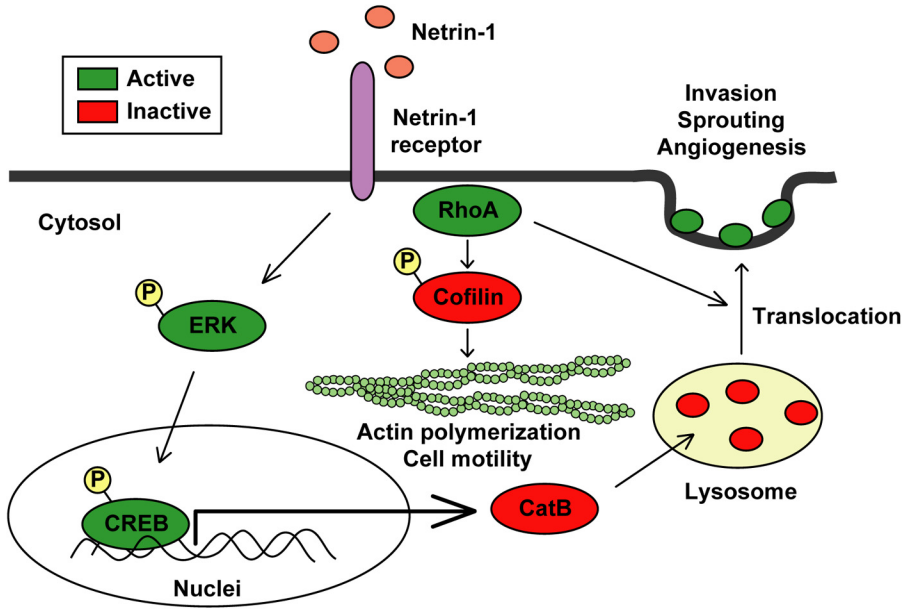

FIGURE 7. **Schematic of netrin-1-dependent pathways.** Netrin-1 activates RhoA (GDP to GTP) in glioblastoma cells and EC, enhancing stress fiber formation and the integrity of the F-actin cytoskeleton. RhoA induces the phosphorylation of cofilin (actin depolymerization factor) to its inactive form, further promoting cytoskeleton integrity. Netrin-1 also induces CREB phosphorylation via the MAPK pathway, leading to up-regulation of CatB expression. Netrin-1 promotes the translocation of CatB from the lysosome to the cell surface as an enzymatically active form in a RhoA-dependent manner. Once at the cell surface, CatB acts to promote glioblastoma invasiveness and angiogenesis.

netrin-1 via UNC5B (11). Disruption of *Unc5B* in mice or in zebrafish increased vessel branching and abnormal navigation, suggesting a negative role for netrin-1 in vasculogenesis (11, 12). These inconsistent results might be a result of the bifunctional nature of netrin-1, which mediates attraction or repulsion, dependent on differential netrin receptor expression levels. The effects of netrins on angiogenesis are even more complex when taking into account that there are three members of the netrin family: netrin-1, netrin-3, and netrin-4 (1, 10). Netrin-4 inhibits angiogenesis via neogenin and UNC5B (40) and suppresses tumor angiogenesis in colorectal cancer (41). On the other hand, netrin-4 is a pro-angiogenic factor during zebrafish development (42). It seems likely that the differential effects of the netrins are dependent on which netrin receptors are being expressed.

Netrin-1 activity is transduced by a set of netrin-1 receptors, including UNC5A-D, neogenin, DCC, and DSCAM. The qRT-PCR analysis of three glioblastoma (U87MG, U343, and U251) cell lines showed that neogenin was the only receptor expressed in all three cell lines. There was no discernible pattern of receptor expression among the different cell lines. However, it should be cautioned that these receptor profiles are generated from glioblastoma cell lines and might not reflect receptor expression in glioblastoma tumors *in vivo*. HUVEC did not appear to express netrin receptors. The dearth of known netrin-1 receptors in EC is puzzling, considering its angiogenesis activity, but is consistent with a previous report that netrin-1 and netrin-4 pro-angiogenic activity is not mediated by any known netrin receptor (14). Netrin-1 is normally expressed in the brain floor plate, where it attracts commissural neurons expressing netrin-1 receptors (10). We found that netrin-1 is also expressed in several glioblastoma cell lines. Some glioblastoma cells express both netrin-1 and netrin-1 receptors, suggesting the possibility of an autocrine functional loop. A recent report demonstrated an autocrine function for netrin-1 in U87MG cells; however, the loop inhibited cell motility (43).

Netrin-1 signaling pathways are of great interest and the subject of much scrutiny. We have identified three factors that contribute to netrin-1 activities, RhoA, CatB, and CREB. RhoA regulated stress fiber formation and cell motility (31, 32). Netrin-1 activated RhoA within minutes, as measured by rhotekin pulldown analysis, with simultaneous enhancement of stress fiber formation as observed by confocal microscopy. Treatment with the RhoA inhibitor C3 transferase blocked netrin-1-induced invasion. Cofilin, an actin depolymerization factor (44), was phosphorylated by netrin-1 and thus was inactive and stabilized the F-actin cytoskeleton. These molecular results in response to netrin-1 are compatible with enhanced migration and invasion.

A novel aspect of our studies is that netrin-1 promotes invasiveness via the cysteine protease, CatB. Glioblastoma invasion is known to involve protease-mediated degradation of the surrounding extracellular matrix (9). Netrin-1 processed pro-CatB into several mature forms and enhanced enzymatic activity. The specific CatB inhibitor CA-074Me inhibited netrin-1-induced glioblastoma cell sprouting and infiltration of blood vessels into Matrigel molds implanted into mice. By comparison, CatD and CatL inhibitors had no effect on these netrin-1 biological activities, and CatS had only a slight effect, suggesting a degree of specificity in the cathepsin family.

One unanswered question was how CatB, a lysosomal enzyme, could be a cell surface or secreted protease. We found, however, that upon netrin-1 stimulation, CatB was translocated to the cell surface of glioblastoma cells. Further evidence for CatB translocation to the cell surface was that ANXA2, a cell surface protein, co-localized with CatB. Cell surface-ANXA2 is

involved in tumor invasion and metalloprotease activation (45, 46). Our results are consistent with previous reports that ANXA2 associates with CatB on the surface of tumor cells (35, 37); however, netrin-1 was not used in these studies. We found that translocation of CatB was RhoA-dependent, suggesting that netrin-1-mediated RhoA activation may affect not only cell migration and invasion but also intracellular trafficking of CatB.

Another novel factor we found to be activated by netrin-1 is CREB. Anti-phosphoprotein antibody arrays revealed that treatment of glioblastoma cells with netrin-1 induced CREB phosphorylation within 10 min. CREB is a transcription factor that is expressed in most tissues and is involved in many cellular processes such as proliferation, differentiation, cell survival, and development (47). CREB has been implicated in the survival and invasiveness of glioblastoma (48). In addition, CREB regulates the expression of metalloprotease and cathepsin family members and contributes to breast and melanoma metastasis (38, 39). VEGF has been reported to induce CREB phosphorylation and to increase CREB transcriptional activity in HUVEC, indicating an important role of CREB in angiogenesis (49). Our knockdown of CREB reduced netrin-1-induced glioblastoma cell invasion, sprouting, and CatB expression. Our results indicate that there are some interactions between RhoA, CatB, and CREB in response to netrin-1. For example, RhoA is needed for translocation of CatB to the cell surface. Furthermore, CREB enhances CatB expression. However, we did not find any direct interactions of RhoA and CREB. Multiple netrin-1 signaling pathways are described in Fig. 7.

SEMA3F is an axon guidance factor that has many properties directly inverse of netrin-1, for example, inactivation of RhoA, activation of cofilin, inhibition of migration, and invasion *in vitro* and inhibition of tumor angiogenesis and metastasis *in vivo* (7, 8). SEMA3F expression was down-regulated in highly metastatic tumor cells (7), whereas plasma netrin-1 levels were significantly increased in tumors (50). A balance of netrin-1 and SEMA3F in glioblastoma cells might be a diagnostic and prognostic biomarker for glioblastoma.

Netrin-1 may promote glioblastoma progression in a dual manner by directly stimulating glioblastoma cell invasion and enhancing tumor angiogenesis. These results might have clinical significance. The most common brain tumors are glioblastoma in adults (Central Brain Tumor Registry of the United States (CBTRUS), 2012). The median survival rate for patients with these tumors is only 12–15 months, a time frame not much changed in the past few decades. This poor prognosis stems in large part from the highly invasive and vascular nature of glioblastoma, which makes therapy extremely challenging. Our results identify a novel netrin-1-dependent pathway that may be key to invasiveness. Targeting mediators such as netrin-1 and CatB may prove promising for brain cancer therapy.

Acknowledgments—We thank Melissa Anderson and Kristin Johnson for preparation of the manuscript and for artwork, and Brendan McNeish for protease assays. We thank Elisabeth Jiang for experimental support.

REFERENCES

1. Mehlen, P., Delloye-Bourgeois, C., and Chédotal, A. (2011) Novel roles for slits and netrins. Axon guidance cues as anticancer targets? *Nat. Rev. Cancer* **11,** 188–197
2. Mehlen, P., and Furne, C. (2005) Netrin-1. When a neuronal guidance cue turns out to be a regulator of tumorigenesis. *Cell. Mol. Life Sci.* **62,** 2599–2616
3. Carmeliet, P., and Tessier-Lavigne, M. (2005) Common mechanisms of nerve and blood vessel wiring. *Nature* **436,** 193–200
4. Klagsbrun, M., and Eichmann, A. (2005) A role for axon guidance receptors and ligands in blood vessel development and tumor angiogenesis. *Cytokine Growth Factor Rev.* **16,** 535–548
5. Miao, H. Q., Soker, S., Feiner, L., Alonso, J. L., Raper, J. A., and Klagsbrun, M. (1999) Neuropilin-1 mediates collapsin-1/semaphorin III inhibition of endothelial cell motility: functional competition of collapsin-1 and vascular endothelial growth factor-165. *J. Cell Biol.* **146,** 233–242
6. Soker, S., Takashima, S., Miao, H. Q., Neufeld, G., and Klagsbrun, M. (1998) Neuropilin-1 is expressed by endothelial and tumor cells as an isoform-specific receptor for vascular endothelial growth factor. *Cell* **92,** 735–745
7. Bielenberg, D. R., Hida, Y., Shimizu, A., Kaipainen, A., Kreuter, M., Kim, C. C., and Klagsbrun, M. (2004) Semaphorin 3F, a chemorepulsant for endothelial cells, induces a poorly vascularized, encapsulated, nonmetastatic tumor phenotype. *J. Clin. Invest.* **114,** 1260–1271
8. Shimizu, A., Mammoto, A., Italiano, J. E., Jr., Pravda, E., Dudley, A. C., Ingber, D. E., and Klagsbrun, M. (2008) ABL2/ARG tyrosine kinase mediates SEMA3F-induced RhoA inactivation and cytoskeleton collapse in human glioma cells. *J. Biol. Chem.* **283,** 27230–27238
9. Rao, J. S. (2003) Molecular mechanisms of glioma invasiveness. The role of proteases. *Nat. Rev. Cancer* **3,** 489–501
10. Lai Wing Sun, K., Correia, J. P., and Kennedy, T. E. (2011) Netrins. Versatile extracellular cues with diverse functions. *Development* **138,** 2153–2169
11. Larrivée, B., Freitas, C., Trombe, M., Lv, X., Delafarge, B., Yuan, L., Bouvrée, K., Bréant, C., Del Toro, R., Bréchot, N., Germain, S., Bono, F., Dol, F., Claes, F., Fischer, C., Autiero, M., Thomas, J. L., Carmeliet, P., Tessier-Lavigne, M., and Eichmann, A. (2007) Activation of the UNC5B receptor by Netrin-1 inhibits sprouting angiogenesis. *Genes Dev.* **21,** 2433–2447
12. Lu, X., Le Noble, F., Yuan, L., Jiang, Q., De Lafarge, B., Sugiyama, D., Bréant, C., Claes, F., De Smet, F., Thomas, J. L., Autiero, M., Carmeliet, P., Tessier-Lavigne, M., and Eichmann, A. (2004) The netrin receptor UNC5B mediates guidance events controlling morphogenesis of the vascular system. *Nature* **432,** 179–186
13. Park, K. W., Crouse, D., Lee, M., Karnik, S. K., Sorensen, L. K., Murphy, K. J., Kuo, C. J., and Li, D. Y. (2004) The axonal attractant Netrin-1 is an angiogenic factor. *Proc. Natl. Acad. Sci. U.S.A.* **101,** 16210–16215
14. Wilson, B. D., Ii, M., Park, K. W., Suli, A., Sorensen, L. K., Larrieu-Lahargue, F., Urness, L. D., Suh, W., Asai, J., Kock, G. A., Thorne, T., Silver, M., Thomas, K. R., Chien, C. B., Losordo, D. W., and Li, D. Y. (2006) Netrins promote developmental and therapeutic angiogenesis. *Science* **313,** 640–644
15. Tadagavadi, R. K., Wang, W., and Ramesh, G. (2010) Netrin-1 regulates Th1/Th2/Th17 cytokine production and inflammation through UNC5B receptor and protects kidney against ischemia-reperfusion injury. *J. Immunol.* **185,** 3750–3758
16. Gerszten, R. E., and Tager, A. M. (2012) The monocyte in atherosclerosis–should I stay or should I go now? *N. Engl. J. Med.* **366,** 1734–1736
17. Kaufmann, S., Kuphal, S., Schubert, T., and Bosserhoff, A. K. (2009) Functional implication of Netrin expression in malignant melanoma. *Cell. Oncol.* **31,** 415–422
18. Rodrigues, S., De Wever, O., Bruyneel, E., Rooney, R. J., and Gespach, C. (2007) Opposing roles of netrin-1 and the dependence receptor DCC in cancer cell invasion, tumor growth and metastasis. *Oncogene* **26,** 5615–5625
19. Dumartin, L., Quemener, C., Laklai, H., Herbert, J., Bicknell, R., Bousquet, C., Pyronnet, S., Castronovo, V., Schilling, M. K., Bikfalvi, A., and Hage-

dorn, M. (2010) Netrin-1 mediates early events in pancreatic adenocarcinoma progression, acting on tumor and endothelial cells. *Gastroenterology* **138,** 1595–1606, 1606e1–8
20. Fitamant, J., Guenebeaud, C., Coissieux, M. M., Guix, C., Treilleux, I., Scoazec, J. Y., Bachelot, T., Bernet, A., and Mehlen, P. (2008) Netrin-1 expression confers a selective advantage for tumor cell survival in metastatic breast cancer. *Proc. Natl. Acad. Sci. U.S.A.* **105,** 4850–4855
21. Fearon, E. R., Cho, K. R., Nigro, J. M., Kern, S. E., Simons, J. W., Ruppert, J. M., Hamilton, S. R., Preisinger, A. C., Thomas, G., and Kinzler, K. W. (1990) Identification of a chromosome 18q gene that is altered in colorectal cancers. *Science* **247,** 49–56
22. Vogelstein, B., Fearon, E. R., Kern, S. E., Hamilton, S. R., Preisinger, A. C., Nakamura, Y., and White, R. (1989) Allelotype of colorectal carcinomas. *Science* **244,** 207–211
23. Llambi, F., Causeret, F., Bloch-Gallego, E., and Mehlen, P. (2001) Netrin-1 acts as a survival factor via its receptors UNC5H and DCC. *EMBO J.* **20,** 2715–2722
24. Austrup, F., Uciechowski, P., Eder, C., Böckmann, B., Suchy, B., Driesel, G., Jäckel, S., Kusiak, I., Grill, H. J., and Giesing, M. (2000) Prognostic value of genomic alterations in minimal residual cancer cells purified from the blood of breast cancer patients. *Br. J. Cancer* **83,** 1664–1673
25. Reyes-Mugica, M., Rieger-Christ, K., Ohgaki, H., Ekstrand, B. C., Helie, M., Kleinman, G., Yahanda, A., Fearon, E. R., Kleihues, P., and Reale, M. A. (1997) Loss of DCC expression and glioma progression. *Cancer Res.* **57,** 382–386
26. Hida, K., Hida, Y., Amin, D. N., Flint, A. F., Panigrahy, D., Morton, C. C., and Klagsbrun, M. (2004) Tumor-associated endothelial cells with cytogenetic abnormalities. *Cancer Res.* **64,** 8249–8255
27. Bielenberg, D. R., Shimizu, A., and Klagsbrun, M. (2008) Semaphorin-induced cytoskeletal collapse and repulsion of endothelial cells. *Methods Enzymol.* **443,** 299–314
28. Coma, S., Shimizu, A., and Klagsbrun, M. (2011) Hypoxia induces tumor and endothelial cell migration in a semaphorin 3F- and VEGF-dependent manner via transcriptional repression of their common receptor neuropilin 2. *Cell Adh. Migr.* **5,** 266–275
29. Smalley, K. S., Lioni, M., and Herlyn, M. (2006) Life isn't flat. Taking cancer biology to the next dimension. *In vitro Cell. Dev. Biol. Anim.* **42,** 242–247
30. Mammoto, A., Connor, K. M., Mammoto, T., Yung, C. W., Huh, D., Aderman, C. M., Mostoslavsky, G., Smith, L. E., and Ingber, D. E. (2009) A mechanosensitive transcriptional mechanism that controls angiogenesis. *Nature* **457,** 1103–1108
31. Burridge, K., and Wennerberg, K. (2004) Rho and Rac take center stage. *Cell* **116,** 167–179
32. Hall, A. (2005) Rho GTPases and the control of cell behaviour. *Biochem. Soc. Trans.* **33,** 891–895
33. Conus, S., and Simon, H. U. (2008) Cathepsins. Key modulators of cell death and inflammatory responses. *Biochem. Pharmacol.* **76,** 1374–1382
34. Mohamed, M. M., and Sloane, B. F. (2006) Cysteine cathepsins. Multifunctional enzymes in cancer. *Nat. Rev. Cancer* **6,** 764–775
35. Cavallo-Medved, D., Dosescu, J., Linebaugh, B. E., Sameni, M., Rudy, D., and Sloane, B. F. (2003) Mutant K-ras regulates cathepsin B localization on the surface of human colorectal carcinoma cells. *Neoplasia* **5,** 507–519
36. Roshy, S., Sloane, B. F., and Moin, K. (2003) Pericellular cathepsin B and malignant progression. *Cancer Metastasis Rev.* **22,** 271–286
37. Cavallo-Medved, D., and Sloane, B. F. (2003) Cell-surface cathepsin B. Understanding its functional significance. *Curr. Top. Dev. Biol.* **54,** 313–341
38. Melnikova, V. O., Mourad-Zeidan, A. A., Lev, D. C., and Bar-Eli, M. (2006) Platelet-activating factor mediates MMP-2 expression and activation via phosphorylation of cAMP-response element-binding protein and contributes to melanoma metastasis. *J. Biol. Chem.* **281,** 2911–2922
39. Shi, Y., Liu, R., Zhang, S., Xia, Y. Y., Yang, H. J., Guo, K., Zeng, Q., and Feng, Z. W. (2011) Neural cell adhesion molecule potentiates invasion and metastasis of melanoma cells through CAMP-dependent protein kinase and phosphatidylinositol 3-kinase pathways. *Int. J. Biochem. Cell Biol.* **43,** 682–690
40. Lejmi, E., Leconte, L., Pédron-Mazoyer, S., Ropert, S., Raoul, W., Lavalette, S., Bouras, I., Feron, J. G., Maitre-Boube, M., Assayag, F., Feumi, C., Alemany, M., Jie, T. X., Merkulova, T., Poupon, M. F., Ruchoux, M. M., Tobelem, G., Sennlaub, F., and Plouët, J. (2008) Netrin-4 inhibits angiogenesis via binding to neogenin and recruitment of Unc5B. *Proc. Natl. Acad. Sci. U.S.A.* **105,** 12491–12496
41. Eveno, C., Broqueres-You, D., Feron, J. G., Rampanou, A., Tijeras-Raballand, A., Ropert, S., Leconte, L., Levy, B. I., and Pocard, M. (2011) Netrin-4 delays colorectal cancer carcinomatosis by inhibiting tumor angiogenesis. *Am. J. Pathol.* **178,** 1861–1869
42. Lambert, E., Coissieux, M. M., Laudet, V., and Mehlen, P. (2012) Netrin-4 acts as a pro-angiogenic factor during zebrafish development. *J. Biol. Chem.* **287,** 3987–3999
43. Jarjour, A. A., Durko, M., Luk, T. L., Marçal, N., Shekarabi, M., and Kennedy, T. E. (2011) Autocrine netrin function inhibits glioma cell motility and promotes focal adhesion formation. *PloS one* **6,** e25408
44. Bamburg, J. R. (1999) Proteins of the ADF/cofilin family: essential regulators of actin dynamics. *Annu. Rev. Cell Dev. Biol.* **15,** 185–230
45. Gerke, V., Creutz, C. E., and Moss, S. E. (2005) Annexins. Linking Ca^{2+} signalling to membrane dynamics. *Nat. Rev. Mol. Cell Biol.* **6,** 449–461
46. Nakayama, H., Fukuda, S., Inoue, H., Nishida-Fukuda, H., Shirakata, Y., Hashimoto, K., and Higashiyama, S. (2012) Cell surface annexins regulate ADAM-mediated ectodomain shedding of proamphiregulin. *Mol. Biol. Cell* **23,** 1964–1975
47. Mayr, B., and Montminy, M. (2001) Transcriptional regulation by the phosphorylation-dependent factor CREB. *Nat. Rev. Mol. Cell Biol.* **2,** 599–609
48. Mantamadiotis, T., Papalexis, N., and Dworkin, S. (2012) CREB signalling in neural stem/progenitor cells. Recent developments and the implications for brain tumour biology. *BioEssays* **34,** 293–300
49. Mayo, L. D., Kessler, K. M., Pincheira, R., Warren, R. S., and Donner, D. B. (2001) Vascular endothelial cell growth factor activates CRE-binding protein by signaling through the KDR receptor tyrosine kinase. *J. Biol. Chem.* **276,** 25184–25189
50. Ramesh, G., Berg, A., and Jayakumar, C. (2011) Plasma netrin-1 is a diagnostic biomarker of human cancers. *Biomarkers* **16,** 172–180